LAWRENCE
LIVERMORE
NATIONAL
LABORATORY

Electron Correlation Effects in Uranium Dioxide from X-ray Emission Spectroscopy

S. W. Yu, J. G. Tobin

September 26, 2012

Disclaimer

This document was prepared as an account of work sponsored by an agency of the United States government. Neither the United States government nor Lawrence Livermore National Security, LLC, nor any of their employees makes any warranty, expressed or implied, or assumes any legal liability or responsibility for the accuracy, completeness, or usefulness of any information, apparatus, product, or process disclosed, or represents that its use would not infringe privately owned rights. Reference herein to any specific commercial product, process, or service by trade name, trademark, manufacturer, or otherwise does not necessarily constitute or imply its endorsement, recommendation, or favoring by the United States government or Lawrence Livermore National Security, LLC. The views and opinions of authors expressed herein do not necessarily state or reflect those of the United States government or Lawrence Livermore National Security, LLC, and shall not be used for advertising or product endorsement purposes.

Electron Correlation Effects in Uranium Dioxide
from X-ray Emission Spectroscopy

SW Yu and JG Tobin*

Lawrence Livermore National Laboratory, Livermore, CA, USA

Abstract

X-ray Emission Spectroscopy (XES) and Bremstrahlung Isochromat Spectroscopy (BIS), two electron-in/photon-out measurements, have been used to probe multi-electronic effects in the important actinide compound, Uranium Dioxide (UO_2). Electron shielding in the $4d_{5/2}$ main and satellite XES peaks are discussed in light of the experimental observations. New XES data for 4f and 4p derived transitions are also presented and discussed.

*Contact Author: Tobin1@LLNL.Gov

Electron Correlation Effects in Uranium Dioxide from X-ray Emission Spectroscopy

Introduction

Whether loved, hated, feared or merely tolerated, actinides are an important part of modern technological society. They play crucial roles in applications that range from smoke detectors [1] to national defense [2], space exploration [3] to electrical power generation. [4] In fact, an immense amount of electricity is generated, with a fairly small carbon-footprint, using nuclear power. This includes about 20% of the electrical grid of the USA [5], 40% in Sweden [6], 55% in Slovakia and 80% in France. [5-8] In nuclear power generation, uranium dioxide (UO_2) is the most commonly used fuel. [9]

Uranium dioxide is also a very interesting material scientifically. UO_2 is part of a larger family of uranium oxides, that spans U_4O_9 ($UO_{2.25}$), U_3O_8 ($UO_{2.67}$) and UO_3 [10-12], as well as the off-stoichiometric $UO_{2\pm x}$, with $x << 1$. [13] In terms of formal charge [14], the uranium atom is U^{+4} with a valence configuration of $5f^2$ and the oxygen atoms are each O^{-2}, with $2s^2 2p^6$. In its neutral metallic state, the uranium valence configuration is $5f^3(spd)^3$. [15] (The spd electrons are associated with the 7s, 7p and 6d orbitals.) While the formal charges in UO_2 suggest a strongly modified electronic structure, it is useful to remember that formal charges are an ionic limit, assuming complete electron transfer to the oxidant. Reality can be quite a bit different, with partial ionization and significant levels of electron sharing. [14, 16] Where uranium dioxide falls still remains a matter of debate, with calculations that suggest both ionicity [17] and covalency. [18]

Electron Correlation Effects in Uranium Dioxide
from X-ray Emission Spectroscopy

Spectroscopically, UO_2 is also complicated. There are multiplets and satellite

structures reported in X-ray Photoelectron Spectroscopy (XPS) [19-22], Inverse

Photoelectron Spectroscopy (IPES)/Bremstrahling Isochromat Spectroscopy (BIS)

[20,23], X-ray Absorption Spectroscopy (XAS) [24-27] and, most recently, Resonant

Inverse Photoelectron Spectroscopy (RIPES) and X-ray Emission Spectroscopy

(XES). [28] (See figures 1 and 2.) This paper extends the work initially reported in

Reference 28, including new spectroscopic observations and an analysis of multi-

electronic shielding in the XES process.

Experimental

The experiments were performed on site at Lawrence Livermore National

Laboratory, using a spectrometer configured to perform spin resolved

photoelectron spectroscopy and inverse photoelectron spectroscopy. [27-31] As

illustrated in Figures 1 and 2, XES/BIS/RIPES are electron-in/photon-out processes,

with different constraints in terms of the energetics and different experimental

sensitivities. The preparation of the UO_2 sample is described in detail elsewhere,

including an exhaustive characterization with XPS and UPS *in situ*. [29] The high

quality and pedigree of the underlying uranium substrate has been demonstrated

previously. [22,29] The technical specifics of the measurements, such as the

monochromator calibration and resolution determination, have been discussed

previously. [30]

Electron Correlation Effects in Uranium Dioxide
from X-ray Emission Spectroscopy

Spectral Results and Discussion

A good example of the XES data collection is shown in Figure 3. [31] Here, the

O1s XES at 524 eV is shown and compared to the O1s XPS and O1s Auger from

Reference 29, in the two insets on the far right and far left.   As can be seen, there is a

strong similarity between all three peaks, perhaps somewhat accidentally. The XPS

is resolution limited, with a natural line-width that is smaller. [29] In the XPS, the

effect of surface degradation with time is also monitored, via spectra taken at both

zero hours and twenty-four hours after in situ cleaning. In the XES and BIS data

collection, the electron gun energy is fixed and then photons are counted over a

finite energy range corresponding to the width of the channel plate. The channel

plate energy width will depend upon the grating chosen and the centroid energy of

the channel plate. In the center of the XES spectrum, one can see a strong O1s peak,

with possible contributions from more than one site. The un-cleaned, oxidized U

sample and the uranium dioxide sample exhibit slightly different line-shapes,

suggesting some slight surface modification with in situ ion etching. Also shown in

the interior inset is an image of the electron counting on the channel plate: this is

the image of a well focused, first order peak. (Reference 31 has more on this issue.)

It has a fairly linear leading edge (lower energy) to the left and a well-defined

crescent shape to the right (higher energy). In a perfect world the images of the

entrance slit on the exit plane of the monochomator would be linear: in reality, the

best that can be obtained are these linear/filled half crescents. (This issue will be

returned to below in the discussion of first order versus second order effects.)

Electron Correlation Effects in Uranium Dioxide
from X-ray Emission Spectroscopy

Finally, the centroid energy was determined by the energy calibration that will be

discussed below: the hv scale correction is only rigid shift, without any other

smaller corrections across the width of the plate.

Another good example of XES and BIS/RIPES data collection across the width

of the channel plate is illustrated in Figure 4. Here the BIS/RIPES and XES near the

$4d_{5/2}$ threshold are shown. [28] These data are plotted without individual

background subtraction. Instead, a single constant has been subtracted from all of

them. (The vertical scale, while of arbitrary units, is the same for all of the spectra,

both XES and BIS/RIPES.) This demonstrates the self-normalization of the

XES/BIS/RIPES data collection. As the electron excitation energy is changed (inset),

the IPES peak shifts linearly. The backgrounds across the channel plate width

remain fairly constant. It is also easy to see the resonances in RIPES that occur at

the photon energies corresponding to the $4d_{5/2}$ main peak and satellite. Again, the

horizontal photon energy scale is that of the original data collection, with a rigid

shift based upon the photon energy calibration, which is discussed next. However,

before going on to that discussion, it is useful to note that the core level

spectroscopy aspect of XES, with the observation of O and U peaks, confirms the

sample composition determination from XPS. [29]

While the original monochromator energy calibration for the G1 grating was

quite good, it was necessary to make a final correction using in situ experimental

data. [30] The most direct way to do this is to use BIS over a wide energy range,

away from any resonances.   The data utilized is shown in Figure 5. [31] Data

Electron Correlation Effects in Uranium Dioxide
from X-ray Emission Spectroscopy

collection time for each spectrum was about 24 hours each. Using the energy

relation shown in Figure 1 and 2, and assuming that the energy corrections scale

with $(hv)^2$, it is possible to extract a single wavelength correction that can then be

applied to all of the spectra, scaled to $(hv)^2$, as described in Reference 30. (This

process remedies a common aliment in ultra-high vacuum monochromators: a small

shift of the energy zero with pump-downs and bake-outs. Another example of this

kind of correction is discussed in Reference 32.) Thus, a single correction, $\Delta\lambda \sim 0.3$

angstroms, is applied universally to the grating 1 energy values. [28,30,31]

An interesting aspect of XES is the non-statisticality of the spin-orbit split

doublet. [30] This can be seen in Figure 6. The XPS of the $U4d_{5/2}$ and $U4d_{3/2}$ peaks

exhibit relative intensities that approximately correspond to their occupation ratio

of 6:4. This is not the case for the XES of the $U4d_{5/2}$ and $U4d_{3/2}$. The $U4d_{3/2}$ is much

weaker, in part because of the possibility of alternate decay pathways, as illustrated

in Figure 2. This effect was previous observed in the XES of cerium oxide as well.

[30] Note that the $U4d_{5/2}$ satellite is actually stronger than the main peak, as

discussed in Reference 28. The observation of non-statisticality will be important in

the discussion of the 4f XES below.

As described above and in Reference 28, there are two XES and RIPES

features each corresponding to the $U4d_{5/2}$ core level: the main peak and the satellite.

(Figure 4) An interesting avenue of interrogation would be to probe the intensity

dependences in the XES as a function of excitation. As seen in Figure 4, for

excitation energies of 1000 eV and 3000 eV, the XES spectra look much the same.

Electron Correlation Effects in Uranium Dioxide from X-ray Emission Spectroscopy

However, what would happen if the excitation were raised sufficiently to access other core levels, opening up the possibility of other decay paths? This question was address for the $U3d_{5/2}$ and $U3d_{7/2}$ core levels (Binding Energies for U of 3552 and 3728 ev, respectively, [33]). Here in the lower panel in Figure 7, as in Figure 4, a single constant value was subtracted from all the spectra and the scaling of the y axis is the same for all of the spectra. Unfortunately, there was no selective enhancement of either peak. However, three new features were observed: Two of them are assigned as loss features associated with a $6p_{1/2}$ to Conduction Band co-excitation. (Binding Energy for U of 27 eV [33]) the third feature is associated with a 5s to $4p_{3/2}$ transition, as will be discussed next.

As in Auger Spectroscopy, threshold determinations can be used to assign peak origins. In the case of the XES peak at a photon energy of 674 eV, the onset occurs between 770 eV and 100 eV. (This is shown in the upper right panel in Figure 7.) The nominal binding energy of the $U4p_{3/2}$ peak in XPS is about 1040 eV, [33] seemingly too high to be associated with a threshold of 1000 eV. However, p core levels can be strange creatures, exhibiting very large broadening effects. [34] A manifestation of this can be seen in the XPS spectrum in the upper left panel of Figure 7. The $4p_{3/2}$ peak is very broad, extending down to the satellite features of the O1s Auger peak. The front tail of the $4p_{3/2}$ transition is in the regime of an effective binding energy of 1000 eV. Thus, the threshold for the $4p_{3/2}$ hole generation would be on the scale of 1000 eV and consistent with the observations in the upper right panel of Figure 7.

Electron Correlation Effects in Uranium Dioxide from X-ray Emission Spectroscopy

At theses energies, XES still tends to be dominated by electric dipole transitions [35], with their $\Delta l = +/- 1$ selection rules. The absence of a doublet suggests no spin-orbit splitting in the decay path. Thus, a 5s to 4p transition is quite likely. Again, the energetics need to be examined closely. The nominal binding energy of the U5s is 321 eV. [33] Using binding energies from XPS, one might expect a photon emitted at hv = 1043 – 321 eV = 722 eV. However, the 5s to 4p transition will occur in the presence of a hole inside the 5s state, closer to the nuclear core. So, the effective nuclear charge for the 5s state will now be increased. The 5s state will collapse around the 4p hole, lowering the energy. If Z = 92 for U, then Z+1 = 93. Based upon an examination of 5s binding energies versus Z for the early actinides and the reduced threshold, it is not unreasonable to expect a shift on the scale of many 10's of eV. Hence, the observed photon energy of 674 eV is plausible. It should also be noted that the 4p full-width at half-maximum is consistent with O1s XES spectrum in Figure 3,using the G1 grating, assuming slight broadening with increasing hv.

Having observed 4d XES, it was decided to probe for the presence or absence of the corresponding 4f XES features. The spectral results of this study are plotted in Figure 8. To summarize, an U4f XES is observed, but is often dominated by U4d features from second order features. To unravel this enigma, it is best to consider the data in Figure 8 from the bottom up.

In order to access the lower energies associated with the 4f transitions (the nominal U4f binding energies are 377 eV and 388 eV [33]), it is necessary to use the

Electron Correlation Effects in Uranium Dioxide
from X-ray Emission Spectroscopy

G2 grating inn the photon detection. [31] When excitation energies near the U3d core levels were used, the spectra in the lowest panel were obtained. Again, a single constant value was subtracted from all of the spectra and the vertical axis is the same for all of the spectra. If one compares the spectra in the lowest panel of Figure 8 with those in the lower panel in Figure 7, it is clear that they are essentially the same, with only a worsening of broadening in the Figure 8 data. The drawback of this is that there are no new effects here. The positive aspect is that it permits a calibration of the G2 grating. As with the case of the G1 grating, the initial calibration of the G2 grating was close, but need fine-tuning. The redundancy in data permitted this fine-tuning of the energy scale.

The worsening of the broadening in the lowest panel of Figure 8 is more than is to be expected from merely going to second order. A consideration of broadening for a fixed entrance slit size, when going from first order to second order, suggests a factor of two worsening. However, this is not sufficient to explain what is observed experimentally. A summary of the observed peak widths is shown in Table 1, illustrating this point. However, it is important to note that resolution arguments are founded upon the assumption that the entrance slit is well-imaged on the detector residing on the exit plane of the monochromator. Soft x-rays can be maddeningly difficult to focus. In our monochromator, the first order soft x-rays are fairly well-focussed, but second order soft x-rays are not. This can bee seen by observing the images of the spectral features on the detector itself. As seen in Figure 3, a fairly well-focussed line has the appearance of a filled half-crescent.

Electron Correlation Effects in Uranium Dioxide from X-ray Emission Spectroscopy

However, a second order feature can be strongly distorted. An example of this for the 5s to 4p transition is shown in the upper panel of Figure 8: the filled half-crescent is gone, replaced by a blurry oval. While this is somewhat disappointing, it is not unreasonable. Considering the approximations that go into soft-x-ray monochromator design, in hindsight, this degradation in second order is not unexpected.

Having achieved an understanding of the spectra in the lowest panel in Figure 8 and calibrated the G2 grating, it is useful to attempt to "turn off" the second order effect by manipulation the excitation energy. The results of this operation are shown in the middle panel in Figure 8. Again, a single constant value was subtracted from all of the spectra and the vertical axis is the same for all of the spectra. As the excitation energy drops below 1000 eV, the 5s to 4p transition disappears, just as it should, thus confirming our assignment. At the same time, the feature near 750 eV in second order and 375 eV in first order does not completely disappear, even for an excitation energy of 700 eV. This suggests that the U4d peaks in second order were overlaying something else near 375 eV in first order.

The nature of this overlap can be best explained by comparing just two of the spectra from the middle panel, as shown in the top panel of Figure 8. The spectrum with the excitation of 2000 eV shows the 5s to 4p transition and the broad U4d feature, encompassing the main 4d feature, its satellite and the underlying lower energy peak. The spectrum excited with 700 eV has no 5s to 4p transition and the other peak has narrowed and possibly shifted and become more symmetrical. This

Electron Correlation Effects in Uranium Dioxide
from X-ray Emission Spectroscopy

peak is assigned as the U4f$_{7/2}$ XES peak. With an observed centroid of about 375 eV,

it is quite consistent with the reported U4f$_{7/2}$ binding energy of 380 eV. [29]

However, the question arises: what about the U4f$_{5/2}$ peak?

As has been observed for the Ce 3d XES [30] and U 4d XES (Figure 6), the

intensities in the spin-orbit split pairs of XES features is not statistical. In fact, the

d$_{3/2}$ features are far weaker and generally broader than the d$_{5/2}$ peaks. Thus, one

might expect that the U4f$_{5/2}$ XES peak would be far weaker and broader than the

U4f$_{7/2}$ XES peak. Using the 2000 eV spectrum in the top panel of Figure 8 as a

background estimate, it is possible to see a broad but real intensity band near 390

eV, consistent with the binding energy of 391 eV. [29, 33] There is even a hint of a

peak structure, but this may be wishful thinking, in light of the observed noise in the

spectrum.

Discussion: Shielding Effects in XES

It is of significance that the satellite in XES occurs at the same energy as the

satellite in RIPES. To address this issue, it is of use to consider the processes in the

main peaks and satellite in XES, IPES and RIPES. Let's start with the equations for

the main or standard feature in XES.

XES 4d$_{5/2}$ Main

$$e(KE^{XES}) + (4d_{5/2})^6(VB\text{-}5f)^2 \rightarrow (4d_{5/2})^5(VB\text{-}5f)^2 + 2e \qquad \text{Eq 1a}$$

$$(4d_{5/2})^5(VB\text{-}5f)^2 \rightarrow (4d_{5/2})^6(VB\text{-}5f)^1 + hv^{XES} \qquad \text{Eq 1b}$$

$$hv^{XES} \approx BE\ (4d_{5/2}) \qquad \text{Eq 1c}$$

VB stands for valence bands and hv is the photon energy.

Electron Correlation Effects in Uranium Dioxide from X-ray Emission Spectroscopy

Next, consider the equations for the simple IPES, with only a direct channel and no indirect channel.

IPES $4d_{5/2}$ Main

$$e(KE^{IPES}) + (4d_{5/2})^6(VB\text{-}5f)^2 \rightarrow (4d_{5/2})^6(VB\text{-}5f)^2(CB\text{-}5f)^1 + h\nu^{IPES} \qquad \text{Eq 2a}$$

$$h\nu^{IPES} \approx KE^{IPES} \qquad \text{Eq 2b}$$

CB stands for conduction band.

RIPES has both a direct and an indirect channel.

RIPES $4d_{5/2}$ Main

<center>Direct</center>

$$e(KE^{RIPES}) + (4d_{5/2})^6(VB\text{-}5f)^2 \rightarrow (4d_{5/2})^6(VB\text{-}5f)^2(CB\text{-}5f)^1 + h\nu^{RIPES}$$

$$\text{Indirect} \qquad \downarrow \qquad\qquad\qquad \uparrow \qquad\qquad\qquad \text{Eq 3a}$$

$$(4d_{5/2})^5(VB\text{-}5f)^2(CB\text{-}5f)^2$$

$$h\nu^{RIPES} = h\nu^{XES} \approx KE^{RIPES} \approx BE\,(4d_{5/2}) \qquad \text{Eq 3b}$$

Next, the satellite for the RIPES will be shown.

RIPES $4d_{5/2}$ Satellite

Here, the subscript S is used to denote the satellite.

<center>Direct</center>

$$e(KE_S^{RIPES}) + (4d_{5/2})^6(VB\text{-}5f)^2 \rightarrow (4d_{5/2})^6(VB\text{-}5f)^2(CB\text{-}5f)^1 + h\nu_S^{RIPES}$$

$$\text{Indirect} \qquad \downarrow \qquad\qquad\qquad \uparrow\ \text{2e transition} \qquad\qquad \text{Eq 4a}$$

$$(4d_{5/2})^5(VB\text{-}5f)^2(CB\text{-}6d)^2$$

$$h\nu_S^{RIPES} = h\nu_S^{XES} \approx KE_S^{RIPES} \approx BE\,(4d_{5/2}) + 2\Delta \qquad \text{Eq 4b}$$

Electron Correlation Effects in Uranium Dioxide
from X-ray Emission Spectroscopy

$\Delta = \varepsilon(\text{CB-6d}) - \varepsilon(\text{CB-5f}) \approx 7 \text{ eV}$ Eq 4c

Δ is the energy (ε) difference between the U5f and U6d manifolds in the UDOS. This

is on the scale of about 7 eV, as discussed in Reference 28. The decay step in the

indirect channel is a two-electron process, with two U6d electrons dropping into the

CB-5f and the $\text{U4d}_{5/2}$ core hole, with the emission of a photon. [28]

The XES satellite should be similar to the RIPES satellite. However, to make it work,

shielding from the spd electrons must be included.

RIPES $4\text{d}_{5/2}$ Satellite

$e(KE^{XES}) + (4d_{5/2})^6(\text{VB-5f})^2(\text{spd})^n \rightarrow (4d_{5/2})^5(\text{VB-5f})^0(\text{spd})^n(\text{CB-6d})^2 + 2e$ Eq5a

$(4d_{5/2})^5(\text{VB-5f})^0(\text{spd})^n(\text{CB-6d})^2 \leftrightarrows (4d_{5/2})^5(\text{VB-5f})^2(\text{spd})^{n-2}(\text{CB-6d})^2$ Eq5b

$(4d_{5/2})^5(\text{VB-5f})^2(\text{spd})^{n-2}(\text{CB-6d})^2 \rightarrow (4d_{5/2})^6(\text{VB-5f})^2(\text{spd})^{n-2}(\text{CB-5f})^1 + hv_S^{XES}$ Eq5c

$hv_S^{RIPES} = hv_S^{XES} \approx BE\,(4d_{5/2}) + 2\Delta'$ Eq5c

$\Delta' = \varepsilon'(\text{CB-6p}) - \varepsilon'(\text{CB-5f}) \approx 7 \text{ eV}$ Eq5d

Here, Δ' and ε' are used to denote the slightly different conditions of XES and RIPES.

Because n is large, the shielding from n-2, n-1 and n should all be roughly

equivalent. This multi-electronic shielding allows us to get back to the transition

through the U6d states and the two-electron transition into the appropriate final

state. It should be noted that 5a is a four-electron process.

Thus, it is clear that our simple pictures of these processes, such as the

main XES peak, bely a more complicated reality, as for the XES satellite peak.

Many electrons are intimately involved in these processes.

Electron Correlation Effects in Uranium Dioxide from X-ray Emission Spectroscopy

Summary and Conclusions

The XES of uranium dioxide has been investigated. While there is a strong satellite in the U4d$_{5/2}$ spectrum, there is no variation or dependence upon changing the excitation energy above threshold or even crossing the U 3d core level energies. New U4f XES peaks have been observed and reported here, as well as a new 5s to 4p transition. While there is a U4d$_{5/2}$ satellite, there is no corresponding U4d$_{7/2}$ satellite: it is unclear why. Perhaps this is a function of the 5f vs. 6d isolation and sensitivity. A consideration of the energetics of the suggests that many electrons are involved in the shielding that would be necessary to get an XES satellite to match the energy of the RIPES satellite.

Electron Correlation Effects in Uranium Dioxide from X-ray Emission Spectroscopy

References

1. http://en.wikipedia.org/wiki/Smoke_detector

2. S.S. Hecker, MRS Bulletin **26**, 672 (2001).

3. http://en.wikipedia.org/wiki/Radioisotope_thermoelectric_generator

4. Y. Guerin, G.S. Was, and S.J. Zinkle, MRS Bulletin **34**, 10 (2009).

5. Nuclear Energy Institute, Nuclear shares of electricity generation,
    http://www.world-nuclear.org/info/nshare.html

6. http://en.wikipedia.org/wiki/Nuclear_power

7. http://www.epa.gov/cleanenergy/energy-and-you/affect/nuclear.html

8. www-pub.iaea.org/mtcd/publications/pdf/pub1304_web.pdf

9. F. Gupta, A. Pasturel and G. Brillant, Phys. Rev. B **81**, 014110 (2010).

10. J.R. Naegele, "Actinides and Some of their Alloys and Compounds," Electronic Structure of Solids: Photoemission Spectra and Related Data, Landolt-Bornstein "Numerical Data and Functional Relationships in Science and Technology," ed. A Goldmann, Group III, Volume 23b, Pages 183 – 327 (1994); and references therein; in particular Figure 115 on page 241.

11. B.W. Veal and D. J. Lam, Phys. Lett. A 49, 466 (1974).

12. E. Thibaut, J.J. Pireaux, J. Riga, C. Tenret-Noel, R. Caudano, E.G. Derouane, and J. Verbist, Proc. 2nd Int. Conf. Electron. Structure of the Actinides, eds. J. Mulak, W. Suski, and R. Troc, Wroclav, Poland, September 13 -16, 1976, p.139.

13. H. Idriss, Surface Science Reports **65**, 67 (2010).

Electron Correlation Effects in Uranium Dioxide
from X-ray Emission Spectroscopy

14. R.E. Dickerson, H.B. Gray and G.P. Haight, "Chemical Principles," 2nd Ed., W.A. Benjamin, Inc., Menlo Park,CA, 1974, page 383.

15. J.R. Naegele, "Actinides and Some of their Alloys and Compounds," <u>Electronic Structure of Solids: Photoemission Spectra and Related Data</u>, Landolt-Bornstein "Numerical Data and Functional Relationships in Science and Technology," ed. A Goldmann, Group III, Volume 23b, Pages 183 – 327 (1994); and references therein; in particular the U summary on page 226.

16. G. Herzberg, "Molecular Spectra and Molecular Structure," Van Nostrand Reinhold Company, New York, NY, 1950.

17. L. Petit et al, Phys. Rev. B **81**, 045108 (2010).

18. I. D. Prodan, G. E. Scuseria, and R. L. Martin, Phys. Rev. B **76**, 033101 (2007)

19. G.C. Allen, I.R. Trickle and P.M. Tucker, Philos. Mag. B **43**, 689 (1981).

20. Y. Baer and J. Schoenes, Solid State Commun. **33**, 885 (1980); Y. Baer and J.K. Lang, Phys. Rev. B **21**, 2060 (1980).

21. B.W. Veal and D. J. Lam, Phys. Rev. B 10, 4902 (1974); Phys. Lett.A 49, 466 (1974).

22. W. McLean, C.A. Colmenares, R.L. Smith and G.A. Somorjai, Phys. Rev. B **25**, 8 (1982).

23. G. Chauvet and R. Baptist, Solid State Commun. 43, 793 (1982).

24. G. Kalkowski, G. K. Kaindl, W. D. Brewer, and W. Krone, Phys. Rev. B **35**, 2667 (1987).

25. F. Jollet, T. Petit, S. Gota, N. Thromat, M. Gautier-Soyer, and A. Pasturel, J. Phys. Condens. Matter. **9**, 9393 (1997).

26. M. Magnuson, S.M. Butorin, L. Werme, J. Nordgren, K.E. Ivanov, J.-H. Guo, and D.K. Shuh, Applied Surface Science **252**, 5615 (2006).

27. S.-W. Yu, J. C. Crowhurst, J. G. Tobin, S. Sharma, J. K. Dewhurst, P. Olalde-Velasco, W. L. Yang, and W. J. Siekhaus, Phys. Rev. B **83**, 165102 (2011).

28. J.G. Tobin and S.-W. Yu, Phys. Rev. Lett, **107,** 167406 (2011).

29. S.W. Yu and J.G. Tobin, J. Vac. Sci. Tech A **29**, 021008 (2011).

30. J.G. Tobin, S.W. Yu, B.W. Chung, G.D. Waddill, L. Duda and J. Nordgren, Phys. Rev B **83**, 085104 (2011).

31. S.-W. Yu, J. G. Tobin, and B.W. Chung, Rev. Sci. Instrum. **82**, 093903 (2011).

32. S.-W. Yu, J. G. Tobin, P. Olalde-Velasco, W. L. Yang, and W. J. Siekhaus, J. Vac. Sci. Tech. A. **30**, 011402 (2012).

33. X-ray Data Booklet, edited by A. Thompson et al. (Lawrence Berkeley National Laboratory, Berkeley, CA, 2001), LBNL/PUB-490 Rev 2.

34. D.A. Shirley, "Many-Electron and Final-State Effects: Beyond the One-Electron Picture," in "Photoemission in Solids I: General Principles," Ed. M. cardona and L.Ley, Springer-Verlag, Berlin, BRD, 1978, page 186.

35. C. Cohen-Tannoudji, B. Diu, and F. Laloe, "Quantum Mechanics," John Wiley and Sons, New York, NY, 1977.

36. R. Jenkins, "Nomenclature in X-ray spectrometry," X-Ray Spectrom. **6**, 104–109 (1977); doi: 10.1002/xrs.1300060212.

Electron Correlation Effects in Uranium Dioxide from X-ray Emission Spectroscopy

Table 1   XES Peak Analysis

Material	Grating	Peak Assignment	hv	Order	SW	ΔE_{FWHM}	ΔE^*_{Prog}
CeOxide	1	RIPES Fermi Edge	885 eV	1st	20μm	2eV	1 eV
CeOxide	1	RIPES Fermi Edge	885 eV	1st	60μm	2eV	3 eV
UO$_2$	1	XES 4d$_{5/2}$ Sat *N5-VB or N5-O6,7*	749	1st	60μm	4eV	2.3 eV
UO$_2$	1	XES 4d$_{5/2}$ Main *N5-VB or N5-O6,7*	735	1st	60μm	3eV	2.2 eV
UO$_2$	1	XES 4p(5s) *N3-O1*	673	1st	60μm	2eV	1.8 eV
UO$_2$	1	XES O1s *K-VB or K-L2,3*	524	1st	60μm	2eV	1.2 eV
UO$_2$	2	XES 4f$_{7/2}$ *N7-VB or N7-P4,5*	374	1st	60μm	2eV	1.1 eV
UO$_2$	2	XES 4d *N5-VB or N5-O6,7*	748	2nd	60μm	7eV	2.2 eV
UO$_2$	2	XES 4p(5s) *N3-O1*	673	2nd	60μm	7eV	1.8 eV

Table Caption
This is a comparison of the various XES features. The experimentally determined values and parameters are shown in the columns to the left. SW is slit width. ΔE_{FWHM} is the experimentally determined full-width-at-half-maximum (FWHM) bandpass or its equivalent. ΔE^*_{Prog} is the energy bandpass predicted by the software running the monochromator and detection system. The first energy resolution measurements are from the RIPES of Cerium Oxide [30] and include the contribution from the excitation, the electron gun. In that study, the gun and detector contributions were extracted wit the result that $\Delta E^*_{Gun}{}^{Extr}$ = 2 eV and $\Delta E^*_{Det}{}^{Extr}$ = 0.35 eV for the 20μm slit width and 1.1 eV for the 60μm slit width. [30] The 4d features have large lifetime broadening and multielectronic effects. The O1s may have a surface and bulk contribution. For second order, the value from the program is estimated by taking the first order prediction and doubling it, as predicted by optical considerations. IUPAC nomenclature has been used in labeling the peaks. [36]

Electron Correlation Effects in Uranium Dioxide
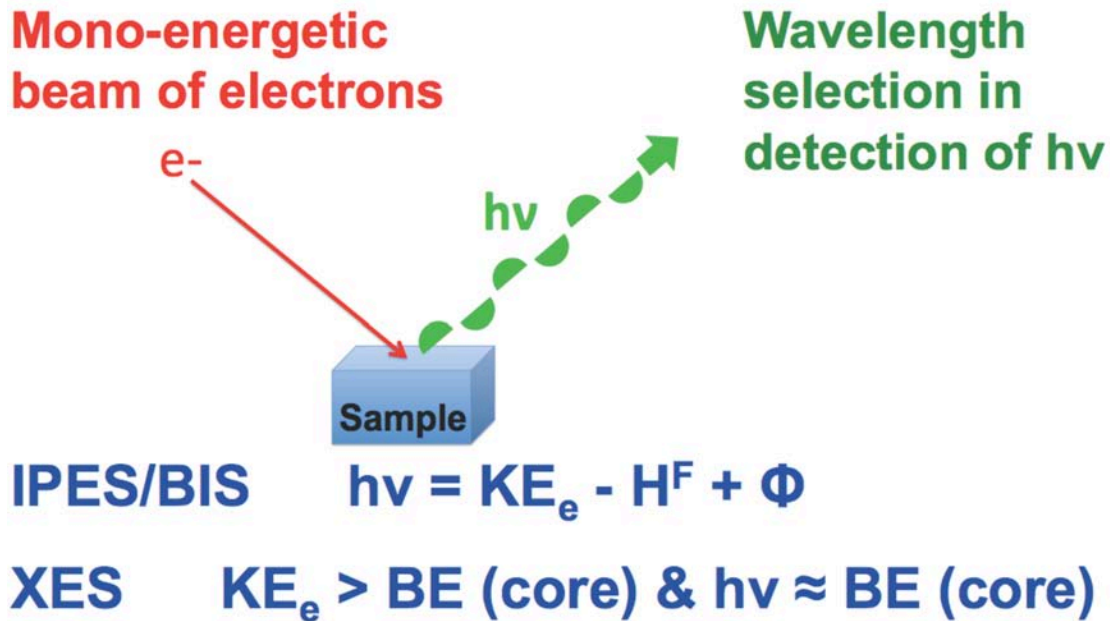# from X-ray Emission Spectroscopy

Mono-energetic beam of electrons

e-

Wavelength selection in detection of hv

hv

Sample

IPES/BIS $h\nu = KE_e - H^F + \Phi$

XES $KE_e > BE\ (core)\ \&\ h\nu \approx BE\ (core)$

Figure 1

A diagram of Experiment of the experiment is shown here. hv is photon energy.

KEe is the energy of the excitation, the electron beam. H^F is the energy of the hole above the Fermi Level. Φ is the work function. BE is binding energy.

Electron Correlation Effects in Uranium Dioxide
from X-ray Emission Spectroscopy
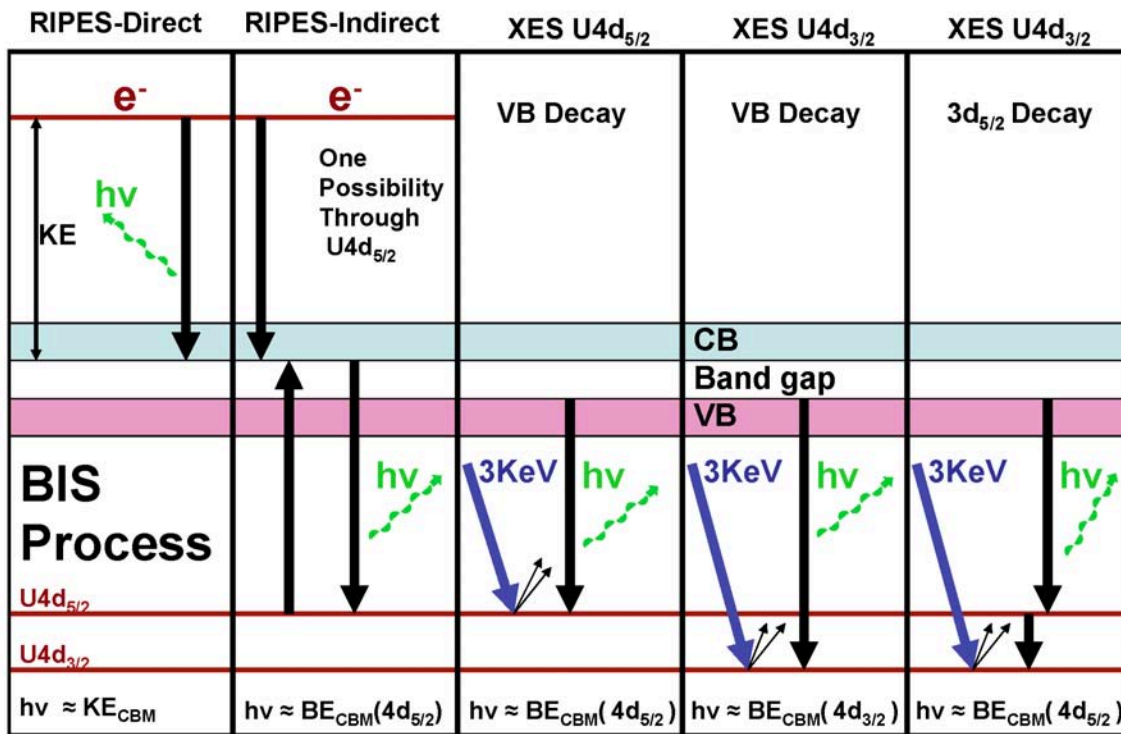
Figure 2

Energy Level Diagram and Experimental Processes, CBM is conduction band

minimum. CB is conduction band. VB is valence band.

Electron Correlation Effects in Uranium Dioxide from X-ray Emission Spectroscopy
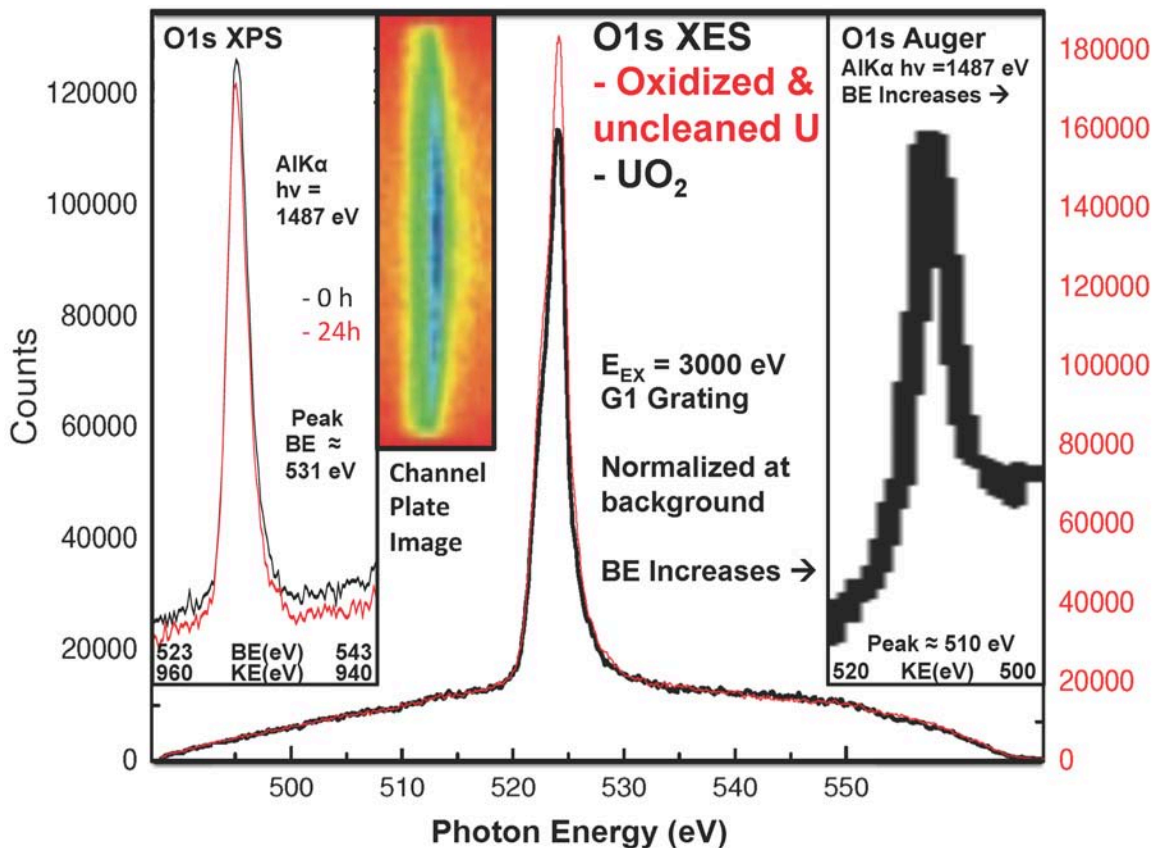
Figure 3

O1s spectra: XES (main figure), Auger (right inset), XPS (left inset) and the channel plate image (central inset).

Electron Correlation Effects in Uranium Dioxide from X-ray Emission Spectroscopy

Uranium Dioxide
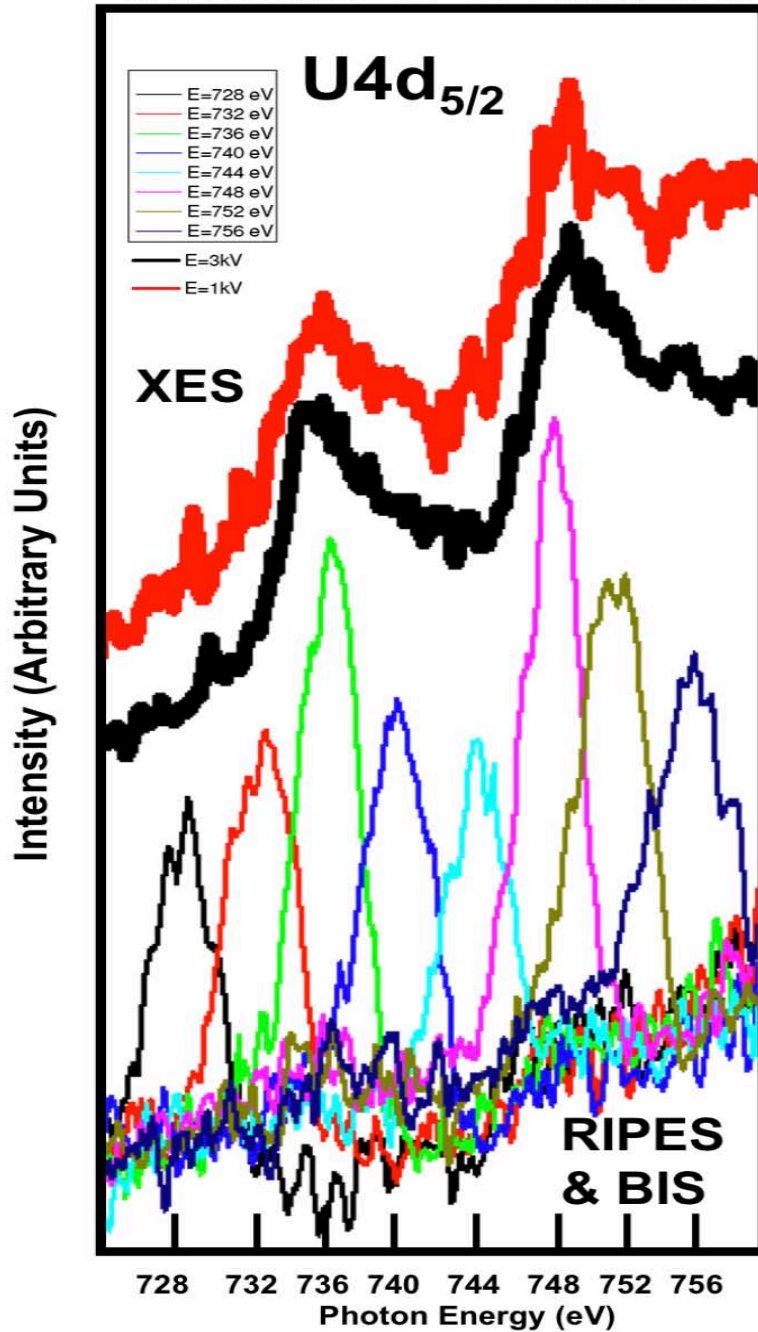
Figure 4

Previous results from RIPES and XES from Reference 29, without individual

background subtraction.

Electron Correlation Effects in Uranium Dioxide
from X-ray Emission Spectroscopy
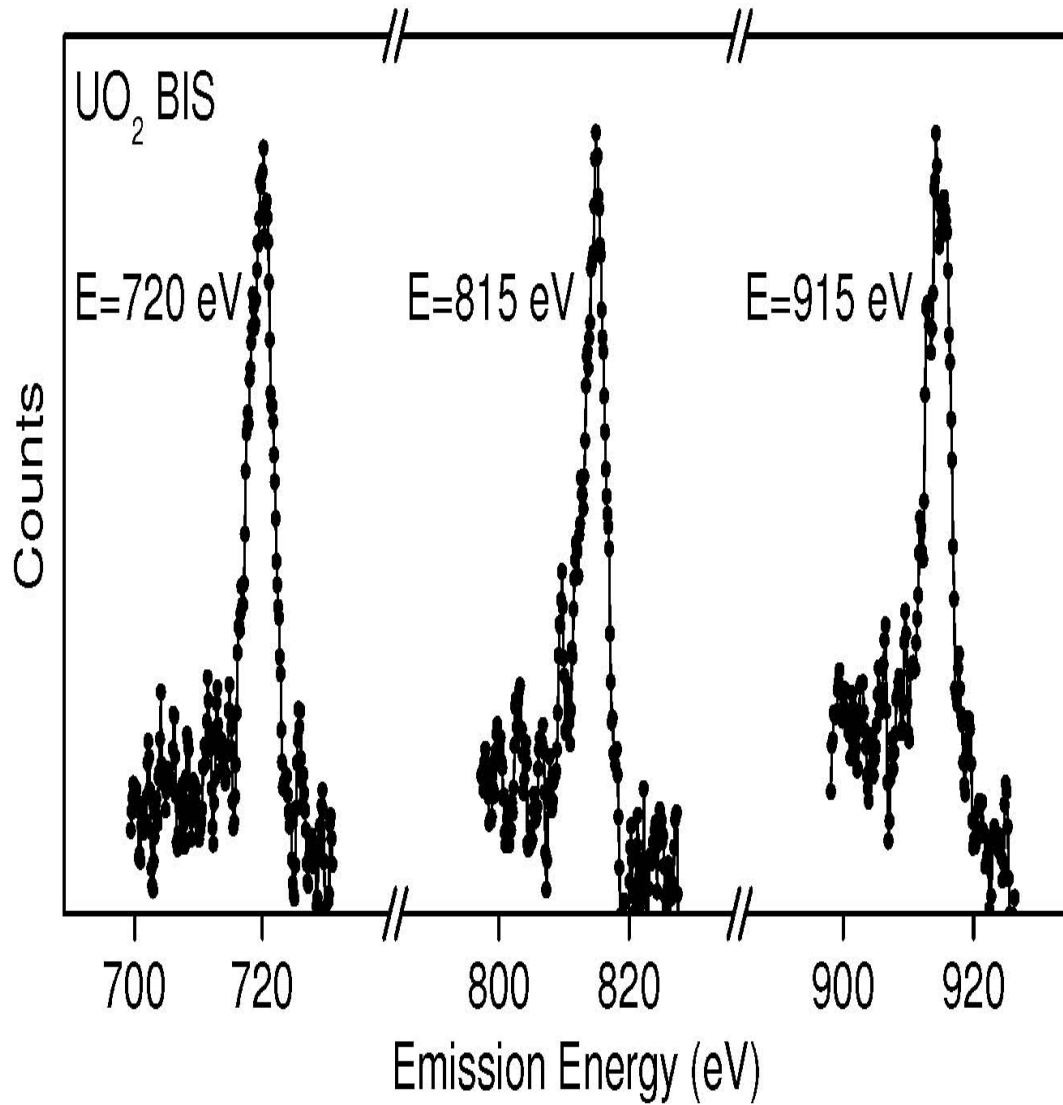
Figure 5

BIS used for the monochromator calibration.

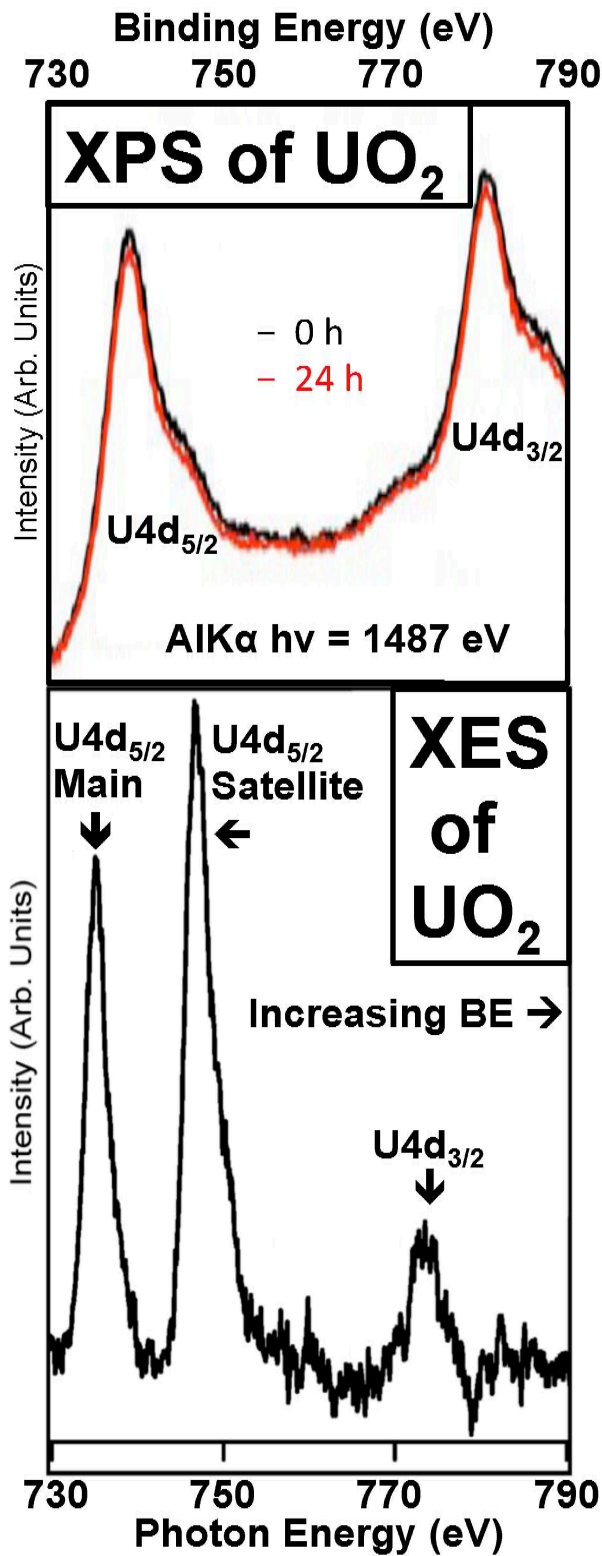# Electron Correlation Effects in Uranium Dioxide
from X-ray Emission Spectroscopy

Figure 6

Here is a comparison of XPS and XES of the U $U4d_{5/2}$ and $U4d_{3/2}$ levels. The XPS spectra include data taken at zero and 24 hours after sample cleaning, as a test of sample stability.

Electron Correlation Effects in Uranium Dioxide
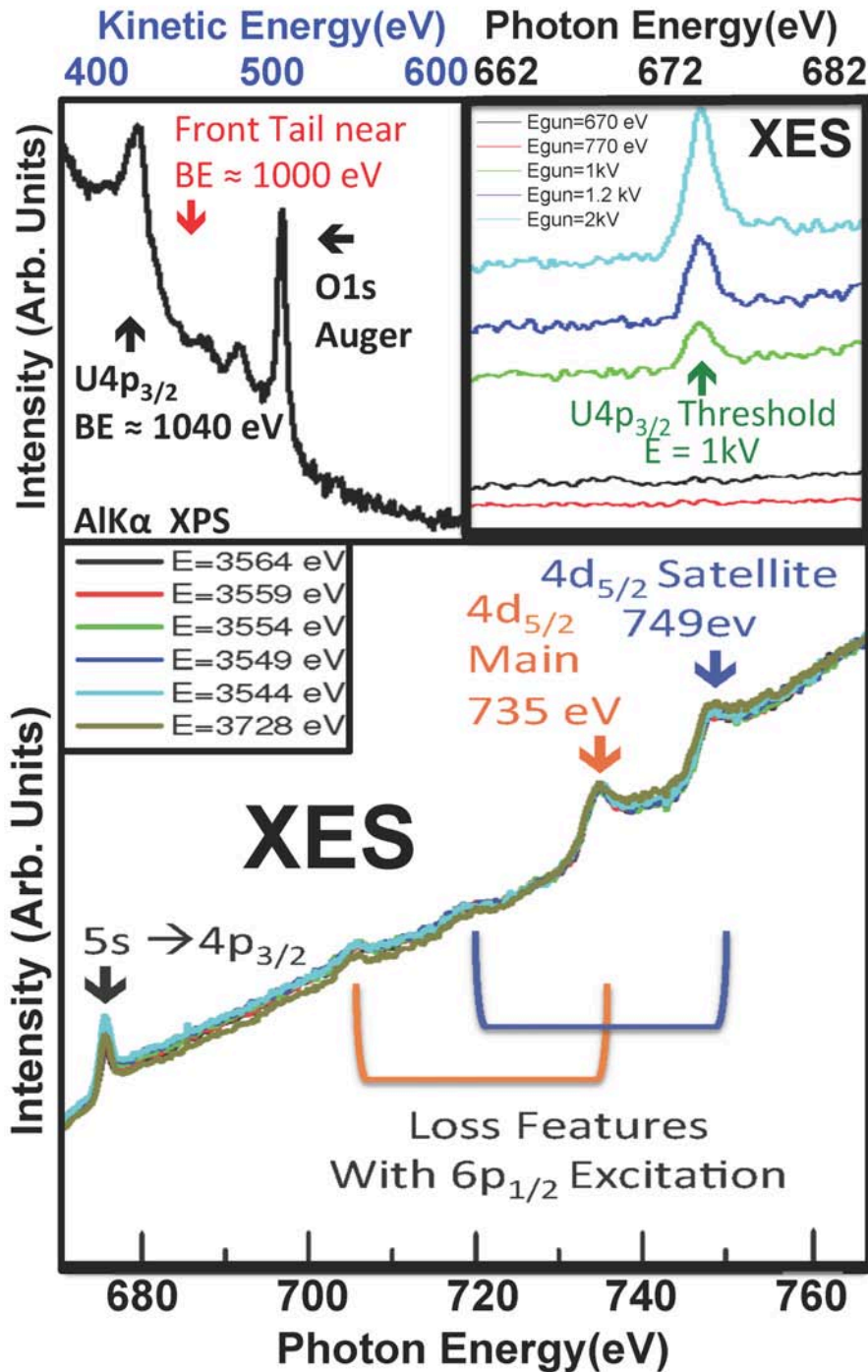## from X-ray Emission Spectroscopy

Figure 7

Lower Panel:

XES of UO_2 in the 4d region, with the excitation KE near 3d edges. The G1 grating was used here.

Upper Right Panel:

XES of UO_2 of the peak near 673 eV as a function of excitation energy. The G1 grating was used here.

Upper left panel:

XPS of UO_2 showing the O1s Auger and $U4p_{3/2}$ features. From Reference 29.

Electron Correlation Effects in Uranium Dioxide
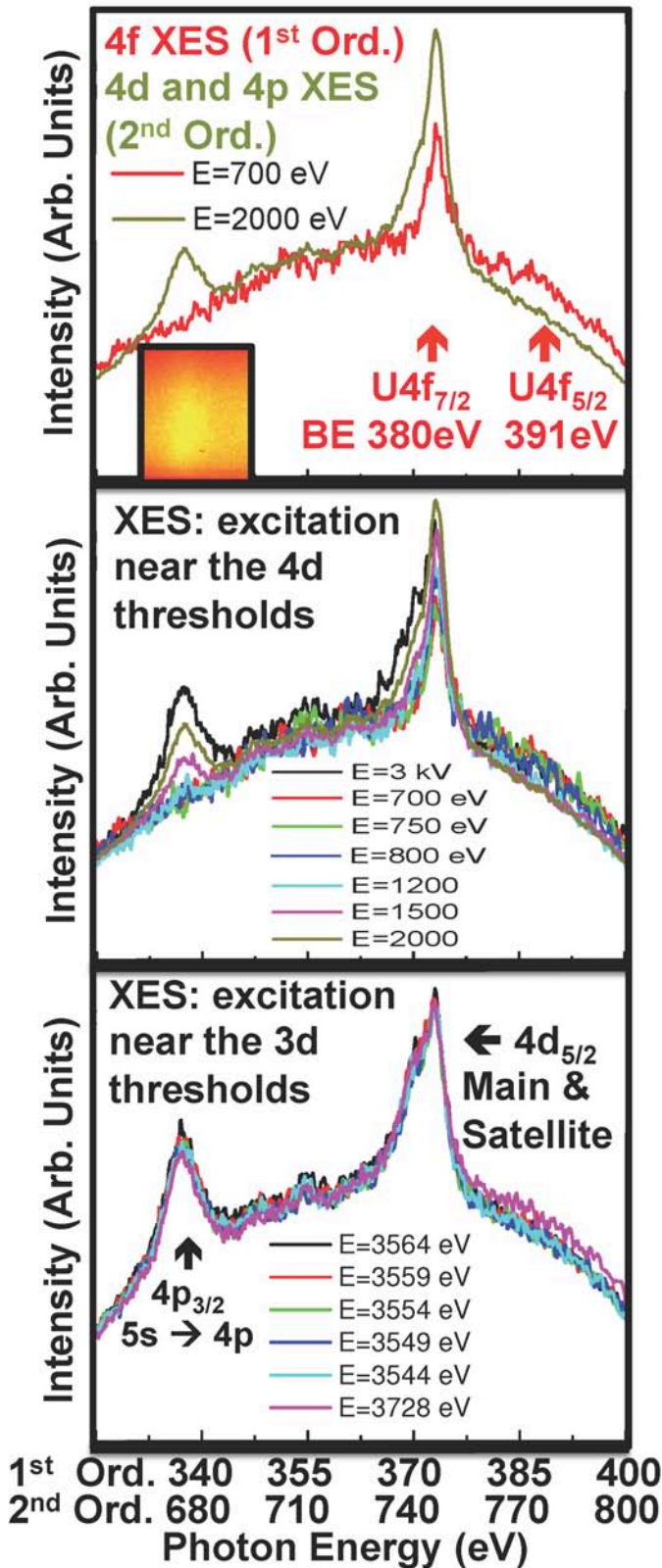## from X-ray Emission Spectroscopy

Figure 8

The XES of UO_2 in 4f region, using the G2 grating calibrated with 2nd order and 4d and 4p XES. See text for details.